

Asymmetry of Frequency Distribution in Power Systems: Sources, Impact and Control

Taulant Kërçi, *IEEE Senior Member*, and Federico Milano, *IEEE Fellow*

Abstract—This letter analyses the sources of asymmetry of frequency probability distributions (PDs) and their impact on the dynamic behaviour of power systems. The letter also discusses on how secondary control can reduce this asymmetry. We also propose an asymmetry index based on the difference between the left and right-hand side standard deviations of the frequency PDs. The IEEE 9-bus system and real-world data obtained from the Irish transmission system serve to show that losses, saturation's and wind generation lead to asymmetric PDs. A relevant result is that the droop-based frequency support provided by wind generation using a tight deadband of 15 mHz leads to significantly increase the asymmetry of the frequency PDs.

Index Terms—Probability distribution (PD), frequency quality, primary frequency control (PFC), active power control (APC), automatic generation control (AGC).

I. INTRODUCTION

The topic of frequency distribution in power systems and the various sources and parameters that influence that has recently received a lot of attention in the literature, in particular, in light of the integration of uncertain and variable renewable energy sources such as wind and solar generation [1]–[4]. The main focus of these works is centred around the modelling, study and reproduction of frequency distribution seen in real grids such as the bi-modal distribution. However, the effect of losses, saturation and renewable sources providing dynamic frequency regulation has not been considered so far. This work fills this gap and provides the following contributions.

- A study of the sources of asymmetry in power systems, such as losses, saturation, and wind generation providing Primary Frequency Control (PFC) and Active Power Control (APC). The latter is a PFC with a tight (15 mHz) deadband [5].
- A metric to quantify the level of asymmetry in power systems. This metric is the difference between left and right standard deviations of the Probability Density (PD) of the system frequency.
- Show through dynamic stochastic simulations and real-world data obtained from the Irish transmission grid that wind generation is a source of asymmetry and that this asymmetry can be reduced with Automatic Generation Control (AGC).

II. POWER SYSTEM MODEL AND METRICS

We model a power system subject to noise as a set of stochastic differential-algebraic equations (SDAEs) [6]:

$$\dot{\mathbf{x}} = \mathbf{f}(\mathbf{x}, \mathbf{y}, \boldsymbol{\kappa}), \quad (1)$$

$$\mathbf{0} = \mathbf{g}(\mathbf{x}, \mathbf{y}, \boldsymbol{\kappa}), \quad (2)$$

$$\dot{\boldsymbol{\kappa}} = \mathbf{a}(\boldsymbol{\kappa}) + \mathbf{b}(\boldsymbol{\kappa}) \circ \boldsymbol{\xi} + \mathbf{c}(\boldsymbol{\kappa}) \circ \boldsymbol{\gamma}. \quad (3)$$

Equations (1) and (2) represent the deterministic part of the dynamic power system. $\mathbf{f} : \mathbb{R}^{l+m+n} \mapsto \mathbb{R}^l$ are the differential equations; $\mathbf{g} : \mathbb{R}^{l+m+n} \mapsto \mathbb{R}^m$ are the algebraic equations; $\mathbf{x} \in \mathbb{R}^l$ is a vector of state variables; $\mathbf{y} \in \mathbb{R}^m$ is a vector of algebraic variables. In (3), $\boldsymbol{\kappa} \in \mathbb{R}^n$ represents the vector of stochastic processes; $\boldsymbol{\xi} \in \mathbb{R}^n$

is a vector of n -dimensional Gaussian white noise that represents the time derivative of the Wiener process; $\boldsymbol{\gamma} \in \mathbb{R}^n$ is a vector of n -dimensional Poisson distributed jumps with normally distributed magnitudes; and \circ represents the element-by-element product of vectors. Stochastic processes are defined by a drift, $\mathbf{a} : \mathbb{R}^n \mapsto \mathbb{R}^n$, and two diffusion terms, $\mathbf{b}, \mathbf{c} : \mathbb{R}^n \mapsto \mathbb{R}^n$.

To evaluate the asymmetry, we propose to calculate the left and right-hand side standard deviations of the frequency PDs, namely “negative” (σ_{f-}) for when the frequency is below the nominal (f_n) (sample size N_-) and “positive” (σ_{f+}) when frequency is above f_n (sample size N_+). Then, we calculate the frequency standard deviation σ_f using a weighted-average method of the two standard deviations (σ_{f-}, σ_{f+}). Next, the asymmetry $\Delta\sigma_f$ is defined as the difference between σ_{f-} and σ_{f+} . These equations are shown below:

$$\sigma_{f-} = \sqrt{\frac{1}{N_-} \sum_{i=1}^{N_-} (f_i - f_n)^2, \{f_i : f_i < f_n\}}, \quad (4)$$

$$\sigma_{f+} = \sqrt{\frac{1}{N_+} \sum_{i=1}^{N_+} (f_i - f_n)^2, \{f_i : f_i > f_n\}}, \quad (5)$$

$$\sigma_f = \sqrt{\frac{1}{N} \sum_{i=1}^N (f_i - f_n)^2} \approx \sqrt{\frac{N_+ \sigma_{f+}^2 + N_- \sigma_{f-}^2}{N_+ + N_-}}, \quad (6)$$

$$\Delta\sigma_f = |\sigma_{f-} - \sigma_{f+}|. \quad (7)$$

Note that the expressions in (6) are substantially equal as, in practice, very few measurements are exactly equal to f_n (e.g., 50 Hz).

Another key metric of frequency quality used by transmission system operators (TSOs) is the so-called 100 mHz criteria which measures the minutes frequency spends outside the ± 100 mHz range [7]. We calculate these minutes in all scenarios below.

III. CASE STUDY

To analyse the statistical properties of the frequency we run long-term time-domain simulations, namely 48h, based on SDAEs [8]. For each scenario, Table I provides relevant information on setup and controllers whereas Table II shows simulation results. The results shown in the remainder of this section are obtained using the IEEE 9-bus system, adapted for the various considered scenarios. All simulations are solved with software tool Dome [9].

A. Power Systems with Conventional Synchronous Generation

In this first section, we focus on the asymmetry that exist in conventional power systems based on synchronous machines. Two potential sources of asymmetry are considered and analysed in detail namely losses and control limiters.

1) *Scenario 1:* This scenario represents conventional power systems with synchronous machines providing both PFC and AGC [10]. The main source of volatility in this scenario is noise in loads modelled as stochastic process that incorporates both continuous and event-driven (jumps) dynamics. This is based on real-world behaviour of loads in the Irish power system [11]. Figure 1(a) depicts the center of inertia frequency PD. As expected, the PD shows a normal/Gaussian distribution and symmetric behavior. These results

T. Kërçi is with EirGrid plc, Transmission System Operator, Dublin, D04 FW28, Ireland. F. Milano is with School of Electrical and Electronic Engineering, University College Dublin, Dublin, D04V1W8, Ireland. E-mails: taulant.kerci@eirgrid.com and federico.milano@ucd.ie.

F. Milano is supported by the Sustainable Energy Authority of Ireland (SEAI) under project FRESLIPS, Grant No. RDD/00681.

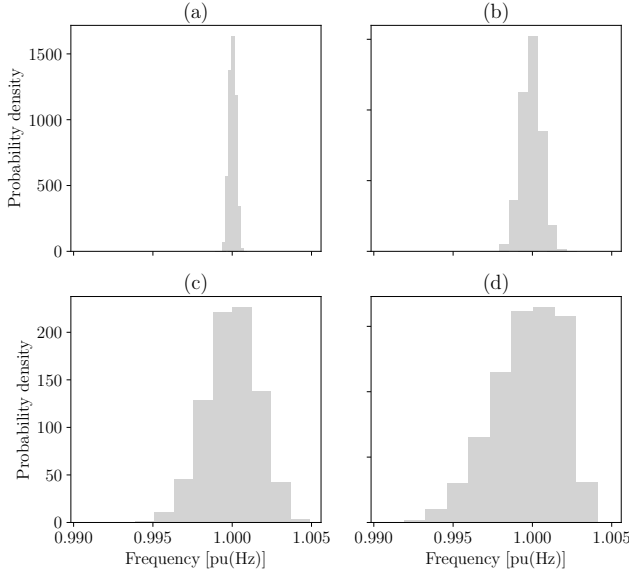


Fig. 1: PD of: (a) Scenario 1, conventional power systems; (b) Scenario 2, losses; (c) Scenario 5, APC and no wind ramps; and (d) Scenario 6, APC and wind ramps.

are confirmed in Table II, which shows that the asymmetry calculated using (7) is small ($\Delta\sigma_f = 0.0001$ Hz) and the minutes outside the 100 mHz range are zero.

2) *Scenario 2*: Here we focus on the impact that the increase of system losses have on the PD. For illustration purposes, we increase the resistance of transmission lines by ten times (this can represent distribution systems). Figure 1(b) shows that losses have a significant impact on the PD and its asymmetry. Moreover, Table II shows that, compared to Scenario 1, $\Delta\sigma_f$ has increased from $\Delta\sigma_f = 0.0001$ Hz to $\Delta\sigma_f = 0.0036$ Hz. Consequently, the standard deviation and the 100 mHz criteria have also increased.

3) *Scenario 3*: In this scenario we simulate the effect of saturation/limits (highly loaded systems). Specifically, we assume that the maximum power of synchronous generator 1 and 2 are reduced by approximately 40% and 50%, respectively. As expected, the results of Table II indicate an increase in the asymmetry in the PD of the frequency compared to, for example, Scenario 1, but lower compared to Scenario 2 that considers high network losses.

B. Power Systems with Non-Synchronous Generation

This section discusses the effect of wind generation and its control under different scenarios. In particular, the aim is to see whether the introduction of wind and its frequency control/regulation capability in the power system affects the asymmetry of the frequency PD. With this aim, we consider again the WSCC 9-bus system and replace the synchronous generator 3 with a wind power plant modelled as a double-fed induction generator [12]. We assume that the wind power plant provides frequency regulation through droop-based PFC with tight deadband namely ± 15 mHz (same used by the governors of conventional generators), as is the case in the Irish power system [7]. This is also known as wind/solar farm APC [5]. To be able to provide up and down regulation, we assume wind is operating 20% below its maximum power point tracking (i.e., curtailed). The description of Scenarios 4-7 is provided in Table I.

1) *Scenario 4*: We assume that wind farms provide frequency regulation only to respond to contingency events (deadband of ± 200 mHz). We also model noise from wind and loads as Gaussian noise, i.e., \mathbf{b} is a constant vector, but no jumps, i.e., $\mathbf{c} = \mathbf{0}$, in (3). Results in Table II indicate that the inclusion of wind farms increase the

asymmetry ($\Delta\sigma_f = 0.0008$ Hz) and minutes outside the 100 mHz range compared to conventional power systems without wind.

2) *Scenario 5*: This scenario considers the effect of wind farms providing APC functionality through the ± 15 mHz deadband. Noise is same as in Scenario 4. Figure 1(c) and Table II show relevant results. Surprisingly, the APC leads to increase σ_f and the asymmetry of the PD (from $\Delta\sigma_f = 0.0008$ Hz to $\Delta\sigma_f = 0.0079$ Hz). These results are a consequence of the nonlinearity of the wind turbine, i.e., the cubic relationship between wind speed and turbine torque.

3) *Scenario 6*: In addition to wind farms providing APC functionality, here we also consider wind ramps modelled based on realistic profile from the Irish power system. Ramps are obtained through stochastic jumps, i.e., \mathbf{c} is not zero, in (3). Results are shown in Table II. The standard deviation ($\sigma_f = 0.1085$ Hz), asymmetry ($\Delta\sigma_f = 0.0386$ Hz) and minutes outside the 100 mHz range (1073.61) have dramatically increased compared to the previous scenario. To illustrate this, we plot in Figure 1(d) the frequency PD. It is striking to see that the behavior of the PD is quite asymmetric.

4) *Scenario 7*: This is same scenario as Scenario 6 but now with AGC. Looking at the results in Table II we can see now that AGC significantly reduces σ_f (from 0.1085 Hz to 0.0794 Hz), the asymmetry (from $\Delta\sigma_f = 0.0386$ Hz to $\Delta\sigma_f = 0.01$ Hz) and minutes outside the 100 mHz range (from 1073.61 to 575.79). Thus, the AGC appears as a viable solution to reduce the frequency asymmetry in power systems and help keep frequency quality within limits.

5) *Scenario 8*: The asymmetry of the frequency PD and dynamic behaviour of the system can be improved further if wind is also providing AGC functionality. This is shown in Table II where we can see that σ_f , $\Delta\sigma_f$ and minutes outside the 100 mHz range are improved significantly with the inclusion of wind farms in AGC.

IV. REAL-WORLD DATA FROM THE IRISH GRID

To validate the previous results, at least for what concerns wind generation and its frequency control, we select three relevant hours of a real-world wind-penetrated system namely the Irish power system with: (i) APC Off (Scenario 9); (ii) APC On (Scenario 10); and different (lower) wind generation levels (Scenario 11). Note that currently in the Irish power system APC is normally disabled. The APC is enabled in special circumstances, e.g., during periods of high export or if there are severe frequency oscillations in the system [5].

In the remainder of this section, we consider three measurement data sets obtained from the TSOs historical information system (coming from SCADA and stored in 1 second resolution) and calculate σ_f , $\Delta\sigma_f$ and minutes outside the 100 mHz range. It is worth mentioning that AGC is not utilized in the Irish power system. Table I summarizes these scenarios. Further information on the operating conditions for each scenario can be found online in [13].

1) *Scenarios 9 and 10*: These two scenarios correspond to the 27 of January 2024, namely 6 consecutive hours, 3 when APC was Off and 3 when APC was turned On. The Irish power system experienced high wind generation around 3.5 GW. Note that the peak demand of the Irish system is just above 7 GW and valley demand is less than 2.5 GW. In these 6 hours, the system non-synchronous penetration was around 72% on average and system conditions remained almost the same, at least, in terms of wind generation, number of conventional units online (i.e., 7) and demand.

Figure 2 depicts the frequency PDs for both scenarios, namely with and without APC. APC Off leads to a normal distribution and symmetric behaviour of the PD. It can be inferred from Table II, in fact, that the asymmetry for the 3 hours when APC was Off is very small and similar to Scenario 1 in the IEEE 9-bus system. The minutes outside the 100 mHz range are also small. It is worth pointing out that whenever the frequency drifts away from the 100

TABLE I: Scenario description for the IEEE 9-bus system and Irish power system.

Scenario	Wind Generation	APC	f_{db_wind} (mHz)	f_{db_conv} (mHz)	AGC conv/wind	Wind Ramps	Load Noise	Wind Noise	Losses	Saturation
1	No	–	–	± 15	Yes _{conv}	No	Yes	–	Normal	No
2	No	–	–	–	No	No	Yes	–	High	No
3	No	–	–	–	No	No	Yes	–	Normal	Yes
4	Yes	Off	± 200	–	No	No	Yes	Yes	Normal	No
5	Yes	On	± 15	–	No	No	Yes	Yes	Normal	No
6	Yes	On	± 15	–	No	Yes	Yes	Yes	Normal	No
7	Yes	On	± 15	–	Yes _{conv}	Yes	Yes	Yes	Normal	No
8	Yes	Off	± 200	–	Yes _{conv&wind}	Yes	Yes	Yes	Normal	No
9	Yes	Off	± 200	± 15	No	Yes	Yes	Yes	Normal	No
10	Yes	On	± 15	± 15	No	Yes	Yes	Yes	Normal	No
11	Yes	Off	± 200	± 15	No	Yes	Yes	Yes	Normal	No

TABLE II: Summary of simulation results for the IEEE 9-bus system and Irish power system.

Scenario	σ_f (Hz)	σ_{f-} (Hz)	σ_{f+} (Hz)	$\Delta\sigma_f$ (Hz)	Minutes Outside ± 100 mHz	Minutes Outside $+100$ mHz	Minutes Outside -100 mHz	P_{loss} (pu)	Q_{loss} (pu)
1	0.0107	0.0108	0.0107	0.0001	0	0	0	0.0409	-0.9452
2	0.0314	0.0330	0.0294	0.0036	5.28	1.27	4.00	0.5097	-0.6151
3	0.0236	0.0245	0.0227	0.0018	0.2233	0.0183	0.205	0.0409	-0.9452
4	0.0602	0.0606	0.0598	0.0008	280.49	136.38	144.10	0.0409	-0.9452
5	0.0803	0.0841	0.0762	0.0079	611.41	287.69	323.71	0.0409	-0.9452
6	0.1085	0.1254	0.0868	0.0386	1073.61	456.67	616.94	0.0409	-0.9452
7	0.0794	0.0845	0.0745	0.01	575.79	267.32	308.47	0.0409	-0.9452
8	0.0635	0.0629	0.0641	0.0012	314.91	152.70	162.20	0.0409	-0.9452
9	0.0558	0.0557	0.0560	0.0003	6.6	3.8	2.8	–	–
10	0.0547	0.0259	0.0575	0.0316	7	7	0	–	–
11	0.030	0.0359	0.0152	0.0207	0	0	0	–	–

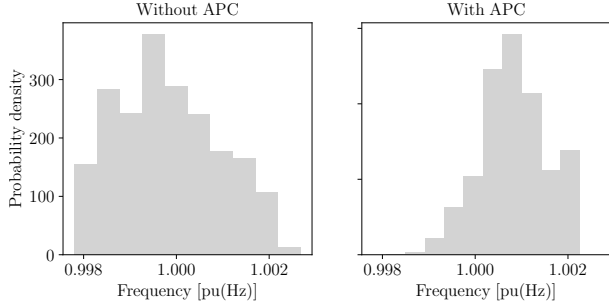


Fig. 2: PD of the Irish power system frequency with and without APC.

mHz range, the operators take manual actions (e.g., conventional generation redispatch) to bring back frequency within the range.

On the other hand, when APC is turned On (all 6 APC groups [5]) to reduce the frequency oscillations is equivalent to Scenario 6. Figure 2 shows that when APC is enabled it seriously increases the asymmetry of the frequency PD. Specifically, it can be seen from the results in Table II that while the average standard deviation (σ_f) is more or less the same with Scenario 9, the asymmetry $\Delta\sigma_f$ has increased dramatically. In fact, the asymmetry is very similar to that considered in Scenario 6 for the IEEE 9-bus system. The asymmetry can also be observed in the minutes outside the 100 mHz range. Note that we tested other real-world scenarios when APC was Off and On and obtained similar results.

2) *Scenario 11*: This last scenario refers to 20th April 2024 and represents a conventional power system with near-zero wind generation as wind levels in the Irish power system during this particular period were around 50 MW. This scenario thus allows for an interesting comparison with respect to the Scenarios 9 and 10 with high wind shares (i.e., 3.5 GW).

Results suggest that σ_f , $\Delta\sigma_f$ and minutes outside the 100 mHz range are reduced compared to Scenario 10. However, compared to Scenario 9, the asymmetry ($\Delta\sigma_f$) is increased significantly. This can be explained by the fact that being a near-zero wind generation condition means that the conventional generators online and inter-

connectors should operate closer to their maximum limits [13].

V. CONCLUSIONS

This paper provides a comprehensive analysis of various sources of asymmetry of frequency PD in power systems. We propose a new metric based on the difference between the standard deviations of the frequency PD to evaluate the system asymmetry. This allows a consistent comparison of asymmetry in different power systems without knowledge of specific parameters and/or system conditions.

REFERENCES

- [1] D. Kraljic, “Towards realistic statistical models of the grid frequency,” *IEEE Transactions on Power Systems*, vol. 38, no. 1, pp. 256–266, 2023.
- [2] D. del Giudice *et al.*, “Effects of inertia, load damping and dead-bands on frequency histograms and frequency control of power systems,” *Int. J. of Electrical Power & Energy Systems*, vol. 129, p. 106842, 2021.
- [3] L. R. Gorrão *et al.*, “Data-driven model of the power-grid frequency dynamics,” *IEEE Access*, vol. 8, pp. 43 082–43 097, 2020.
- [4] P. Vorobev *et al.*, “Deadbands, droop, and inertia impact on power system frequency distribution,” *IEEE Transactions on Power Systems*, vol. 34, no. 4, pp. 3098–3108, 2019.
- [5] EirGrid & SONI, “Active power control groups,” 2020. [Online]. Available: <https://www.sem-o.com/>
- [6] F. Milano *et al.*, “Power system modelling as stochastic functional hybrid differential-algebraic equations,” *IET Smart Grid*, vol. 5, no. 5, pp. 309–331, 2022.
- [7] T. Kërçi *et al.*, “Frequency quality in low-inertia power systems,” in *IEEE PES General Meeting*, 2023, pp. 1–5.
- [8] F. Milano *et al.*, “A systematic method to model power systems as stochastic differential algebraic equations,” *IEEE Transactions on Power Systems*, vol. 28, no. 4, pp. 4537–4544, 2013.
- [9] F. Milano, “A Python-based software tool for power system analysis,” in *IEEE PES General Meeting*, 2013, pp. 1–5.
- [10] T. Kërçi *et al.*, “On the impact of discrete secondary controllers on power system dynamics,” *IEEE Transactions on Power Systems*, vol. 36, no. 5, pp. 4400–4409, 2021.
- [11] F. M. Mele *et al.*, “Modeling load stochastic jumps for power systems dynamic analysis,” *IEEE Transactions on Power Systems*, vol. 34, no. 6, pp. 5087–5090, 2019.
- [12] F. Milano, *Power System Modelling and Scripting*. London, UK: Springer, 2010.
- [13] EirGrid, “Real time system information,” 2024. [Online]. Available: <https://www.eirgrid.ie/grid/real-time-system-information>